

*Steering the self-assembly of octadecylamine monolayers on mica
by controlled mechanical energy transfer from the AFM tip*

J.J. Benítez¹, J.A. Heredia-Guerrero¹ and M. Salmeron².

¹Instituto de Ciencia de Materiales de Sevilla. Centro Mixto CSIC-Universidad de Sevilla. Centro de Investigaciones Científicas Isla de la Cartuja. Avda. Americo Vespuccio 49, 41092 (Sevilla). Spain.

²Materials Sciences Division, Lawrence Berkeley National Laboratory, Berkeley, USA, and Materials Science and Engineering Department, University of California, Berkeley, USA

ABSTRACT.

We have studied the effect of mechanical energy transfer from the tip of an Atomic Force Microscope on the dynamics of self-assembly of monolayer films of octadecylamine on mica. The formation of the self-assembled film proceeds in two successive stages, the first being a fast adsorption from solution that follows a Langmuir isotherm. The second is a slower process of island growth by aggregation of the molecules dispersed on the surface. We found that the dynamics of aggregation can be altered substantially by the addition of mechanical energy into the system through controlled tip-surface interactions. This leads to either the creation of pinholes in existing islands as a consequence of vacancy concentration, and to the assembly of residual molecules into more compact islands.

Keywords: octadecylamine monolayers, self-assembly, AFM, packing defects.

INTRODUCTION.

The formation of self-assembled layers of long chain functionalized alkyl molecules has been studied extensively using scanning probe techniques, mostly for alkane-thiols on gold substrates. Atomic Force and Scanning Tunneling Microscopies (AFM and STM), as well as diffraction techniques, have been used to characterize a series of close packed structures ^{1,2,3,4,5,6}. In the well studied system of alkylsilanes on SiO_x, diffraction measurements have revealed no crystalline order but a short range liquid-like one,^{7,8} with similar results for n-octadecyltriethoxysilane (OTE) on mica ^{9,3}.

Alkane-thiols molecules are strongly attached to the gold substrate through covalent Au-S bonds (154 kJ/mol)^{10,11}. In the case of alkylsilanes on mica the bonding between molecules and support is weaker due to the lack of hydroxyl groups on the mica surface. Some of the cohesive energy of OTE layers is provided by intermolecular Si-O-Si cross-linking, at least between some neighboring siloxane molecules.

In the case of alkylamines (R-NH₂) on mica, the interaction with the substrate is also weak, comparable to the strength of hydrogen bonding (20 kJ/mol). This low cohesive energy is the reason for the unsuccesful attempts to obtain lattice resolution images with AFM¹². However, some structural information has been then derived indirectly by combining topographic data (island height) and a chain interlocking closed packed structural model ^{13,14,15,16}. In spite of this limitation, alkylamines on mica constitute a dynamic system showing interesting phenomena, including molecular and island diffusion, segregations and spontaneous structural modifications (tilting) upon ripening in air ^{12,16,17}.

In a previous paper¹⁶ we reported that alkylamine SAM formation on mica can be described as a two stage process. The first one is relatively fast and comprises

molecular adsorption on the substrate through an acid-base reaction, a process that is determined by the interaction between the amino end group and the adsorption site. The second stage is the much slower diffusion and aggregation of the adsorbed molecules into self-assembled islands. This second stage is dominated by the attractive van der Waals interactions between alkyl chains and, consequently, is faster for longer chain alkylamines. In humid environments this diffusion-aggregation stage is followed by another very slow process characterized by molecular tilting within the islands as water that from the environment penetrates in the islands and protonates the amino groups. We proposed that the resulting electrostatic repulsion is responsible for the observed changes in molecular orientation.

The present study is focused on the two first stages, before molecular tilt takes place. In addition to describing the adsorption and aggregation stages we explore the modifications in the dynamics of the process introduced by the controlled perturbation exerted by the tip of the AFM operating in an intermittent contact mode, also called jumping mode.

EXPERIMENTAL.

Chloroform solutions (Panreac >99.8% stabilized with 50 ppm amylene), were prepared using octadecylamine ($C_{18}-NH_2$) (Fluka, >99%) as received. Muscovite mica samples (New York Corp.) of approx. 8mm x 10mm were double cleaved at room conditions (20-25°C and 45-55% RH) using adhesive tape and immersed in the solution for 1 minute. They were subsequently removed from the solution without rinsing and dried under a gentle dry synthetic air flow for 2-3 minutes. Before imaging the sample specimens were left for 24 hours inside a hermetic test tube previously flushed with dry

air. Further sample ripening at room conditions took place on the microscope sample holder within the volume protected by the AFM glass cover.

A Topometrix Explorer (TMX2000) atomic force is used for all experiments. To ensure that images were representative of the whole sample a large range scanner (130 μm x 130 μm) was used. Sample preparation was repeated twice and data were collected from three distant points. The AFM was operated in contact mode using the same lever (Park sharpened V-shaped Microlever with $k=0.05\text{ N/m}$) and with set points close to the pull-off point, to ensure minimal pressure of the tip. Under these conditions no visible damage to the octadecylamine SAM islands was observed. Both topographic and lateral force images are acquired.

Controlled mechanical perturbation experiments were performed by intermittent contact (jumping mode imaging) using a rectangular Olympus RC800PSA lever with $k=0.1\text{ N/m}$ in a Nanotec Cervantes AFM¹⁸. The vertical load exerted by the tip on the molecular islands was controlled by pre-setting the amplitude of the approach / retract curves. The pull-off force was estimated to be 9.1 nN on mica and 4.2 nN on the top of the islands. Both topographic and adhesion force images were simultaneously obtained. Several approach/retract cycles (from 4 to 10) were averaged at every point of the 256 x 256 matrix of the 10 μm x 10 μm images.

For distance calibration we used a NT-MDT TGT01 silicon grating (2.12 μm pitch) for the X and Y directions, and a Nanosensor H8 certified grating with 7.0 nm step height for the Z direction. Images have been processed and analyzed using the WSxM software from Nanotec¹⁹.

RESULTS AND DISCUSSION.

1. Adsorption, packing and ripening of octadecylamine SAM

Octadecylamine films were prepared from chloroform solutions of increasing concentration. The effect of concentration in the topographic AFM images is shown in figure 1. At low concentration, small scattered islands were formed while at the high concentration both island concentration and their interconnection was higher. In all cases, the surface coverage progressively increased with ripening time after emersion, as shown in figure 1B. After ripening for a week, the island coverage increased by about a factor four if prepared from a 0.25 mM solution, and by about 10% when the concentration was 20mM. These observations can be explained by the presence of an undetectable fraction of adsorbed octadecylamine molecules not yet assembled into islands after short ripening times. These molecules diffuse until they stick and incorporate into an existing island. Both the probability for nucleation and for reaching an existing island is smaller when prepared from diluted solutions, resulting in a slow assembly process. These results indicate that determination of the coverage from AFM images requires ensuring that complete ripening has been reached, a process can take several days. Using this saturation coverage θ_c , the adsorption and assembly on the surface of mica from the solution can be described by a Langmuir isotherm [1] (figure 1C)

$$1/\theta_c = 1 + 1/bc \quad [1]$$

where (b) is a constant proportional to $\exp(-\Delta H_{\text{ads}}/RT)$, and (c) the solution concentration. The value of θ_c was estimated to be 54%. As can be seen in figure 1C the obtained graph is reasonably linear, with a Y axis intercept of 1.02 ± 0.03 , close to the theoretical value of 1 in equation [1]. A similar Langmuir type behavior has been observed for the adsorption and assembly of long chain hydroxyl carboxylic acids²⁰.

Besides the increase in coverage the island morphology also changes upon ripening. As can be observed in figure 1A, the islands aggregate into larger ones. To follow this aggregation process, we have analyzed their area to perimeter (A/P) ratio, which for circular islands corresponds to half the radius. Average A/P values grow with ripening time as shown in figure 2. The slope of such linear plot is progressively smaller as the concentration of the preparation solution is raised. This means that island aggregation by ripening is faster in samples prepared from low concentrations. Topographic data reveal that island displace as an entity and stick to others with no significant contribution from an Ostwald mechanism in which small islands disappear and molecules are transferred to bigger ones.

2. Mechanical interaction between tip and octadecylamine SAM

In previous work we have shown that octadecylamine SAM on mica can be easily eroded by the tip even at external loads close to zero, or when the scanning speed is reduced¹⁵. Unmodified contact mode AFM images can only be obtained when working at negative loads, close to the pull-off point. Since most of the erosion in contact mode is caused by the lateral displacement of the tip over the surface, rather than by the normal load, the jumping mode imaging is ideal to minimize the damage because the lateral displacement of the tip is done out of contact¹⁸. More importantly, the interaction between tip and SAM in jumping mode can be controlled by changing parameters such as the amplitude of the approach/retract cycle, number of cycles per point and number of points per line. In this section, we examine the effect of such mechanical interaction between tip and surface.

Figure 3 shows different topographic changes induced by scanning octadecylamine SAM islands in contact mode compared with the jumping mode. The

top 25% of the image in Fig. 3A is scanned in contact mode at 0.5nN external applied load. Scanning is then stopped and jumping mode activated with the same 0.5 nN set point. The tip is moved back to the upper left corner and the whole image is obtained. The white horizontal line marks the limit between the regions previously imaged in contact mode and the rest. As can be seen, just a single scan in mild contact mode is enough to create tiny holes. No such holes are observed in the jumping mode part of the image.

To explore the response of octadecylamine film to the perturbation exerted by the tip getting in and out of contact, the region marked in figure 3A by a square box was scanned repetitively in jumping mode after increasing the set point to 2 nN, figure 3B. As can be observed, the tip is inducing formation of bridges connecting islands at points of close proximity (marked by arrows), as well as increasing their size by filling in previously empty regions. Island growth induced by the tip is much faster than that observed by mere ripening, as can be seen in figure 3C by comparing the central area, scanned in the previous experiment, with its surroundings and with the starting image shown in the box of figure 3A. The increment in surface coverage in this case is about 17%. As a reference, surface coverage increment for this sample in the whole 7 days of ripening is about 10%. On the other hand, no modification of the height of the islands is observed after successive scans in jumping mode. Therefore, the observed coverage increase cannot be interpreted as the result of molecular tilting as previously observed for much longer ripening times¹⁶.

An additional interesting observation is the increase in the amount of pinholes visible in successive imaging. In figure 4, the evolution of the total number of pinholes as a function of accumulated number of scans is shown. We propose that pinholes are created by the lateral diffusion and agglomeration of vacancies induced by the tip

(scheme I). Both parameters, surface coverage and number of pinholes, display a similar linear trend (inset in figure 4), showing that their origin is directly related, even if no coverage increase should be expected from the vacancy concentration mechanism proposed above. This can be explained by the following simple model. We assume that a fraction of the adsorbed molecules are not incorporated into the islands visible in the images. These molecules might be trapped on defects, or weakly bound to the surface probably lying nearly flat. At room temperature the mobility of these molecules is low. Although heating might activate diffusion, the weak binding might also give rise to evaporation. We propose that the “hammering” action of the tip in the jumping mode is providing the energy that shakes the molecules out of their binding sites and thus enhancing their diffusion and aggregation into islands. The same hammering action can provide the energy for diffusion of vacancies inside the islands leading to pinhole formation. The two processes are acting in parallel is this is the reason for the linear relationship observed between the surface coverage increment and the number of pinholes created.

Figure 5 shows adhesion force maps obtained before and after several successive scans in jumping mode. Bright areas of high adhesion correspond to exposed mica while darker areas correspond to the islands where adhesion is low. While no modification of adhesion is observed on the octadecylamine islands (squares data points in the graph below), two well differentiated adhesion change patterns can be observed on the mica background (circle data points). The areas marked by white arrows are characterized by a strong island aggregation and show an increasing adhesion with the number of accumulated scans. The opposite behavior is observed for mica regions encircled by islands (such as the one marked by the grey arrow). The increasing adhesion on mica is interpreted as “cleaning” process in which residual, not yet self-

assembled octadecylamine molecules are induced to diffuse out of the region, as shown in Scheme I. Scanning in jumping mode is therefore activating and accelerating the molecular motion, which spontaneously would occur in a much longer timescale. It is possible that some of the changes might occur by transfer of molecules from the surface to the tip and from the tip back to the surface.

CONCLUSIONS.

The formation of self assembled monolayers of octadecylamine on mica is a dynamic process ruled by several competing interactions. One is that of the amino end group and the support, where water plays also a role by protonation of the amine groups. Another is the van der Waals interaction between alkyl chains and mica that favors flat adsorption at low coverage. Finally there are van der Waals attraction forces between the molecules. Two consecutive time stages in the self-assembly have been detected. First, molecules adsorb from solution and diffuse rapidly to form islands. This process can be described by a Langmuir isotherm. Secondly, already formed octadecylamine SAMs continue to grow at a slower rate due to diffusion of loosely bound molecules between the islands.

The competition between the various forces mentioned above can be significantly altered by external energy added to the system. We have shown that the “hammering” of the surface by the tip induces an acceleration of some of the dynamic self-assembly processes. It can create pinholes by enhancing the displacement of vacancies. It can also excite loosely bound molecules lying between islands to diffuse and assemble.

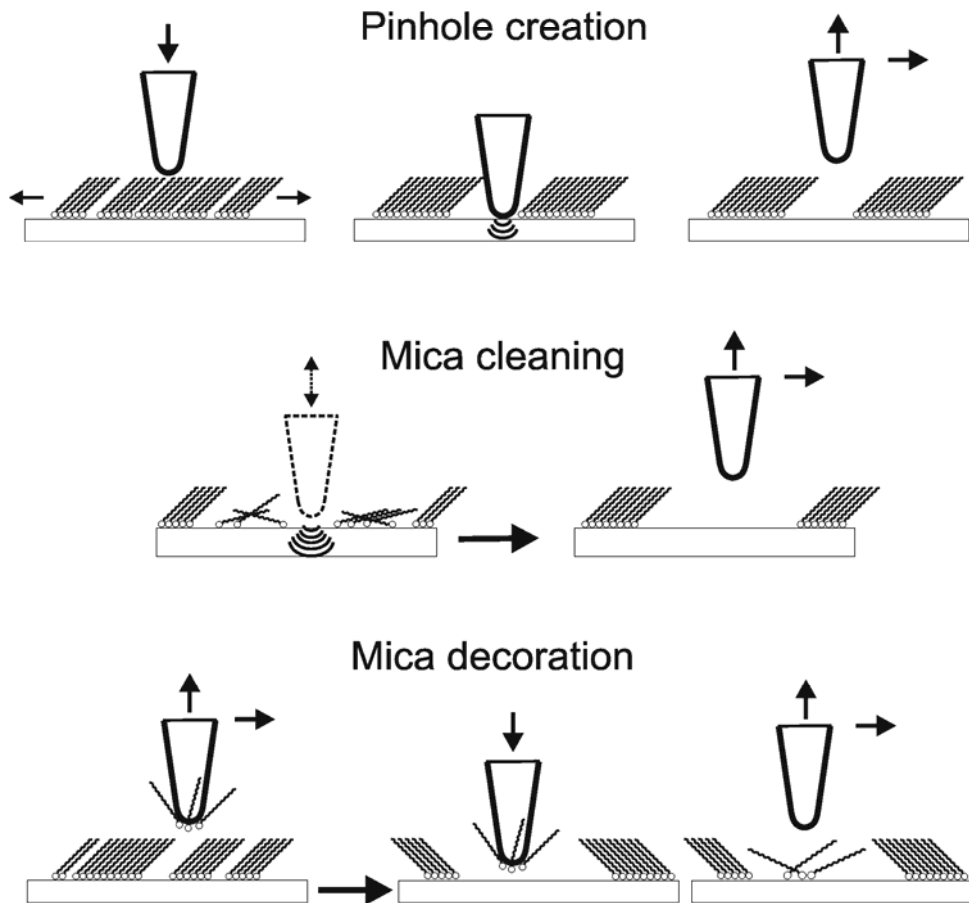
Finally the tip may also contribute directly by shuttling molecules from one location to another, although this process has not been studied in detail.

Our results provide new insights on how energy dissipation between contacting bodies takes place and on the effects of such energy transfer.

Acknowledgments

Funding is provided by Spanish *Ministerio de Ciencia e Innovación* under project CTQ2008-00188. MS is supported by the Office of Science, Office of Basic Energy Sciences, Materials Science and Engineering of the U.S. Department of Energy under Contract No. DE-AC02-05CH11231.

Scheme I



Scheme I. Schematics of processes resulting in pinhole creation inside islands, and cleaning and decoration in regions between islands. We propose these processes to be enhanced by mechanical energy transfer when scanning octadecylamine SAMs on mica in intermittent contact (jumping mode). Top: pinhole created as the tip activates vacancy diffusion and aggregation. Middle: Diffusion of loosely bound molecules on mica regions between islands. These molecules aggregate to the existing islands. Bottom: Molecules attaching to the tip can be transferred to bare mica substrate regions (decoration effect).

Figure 1

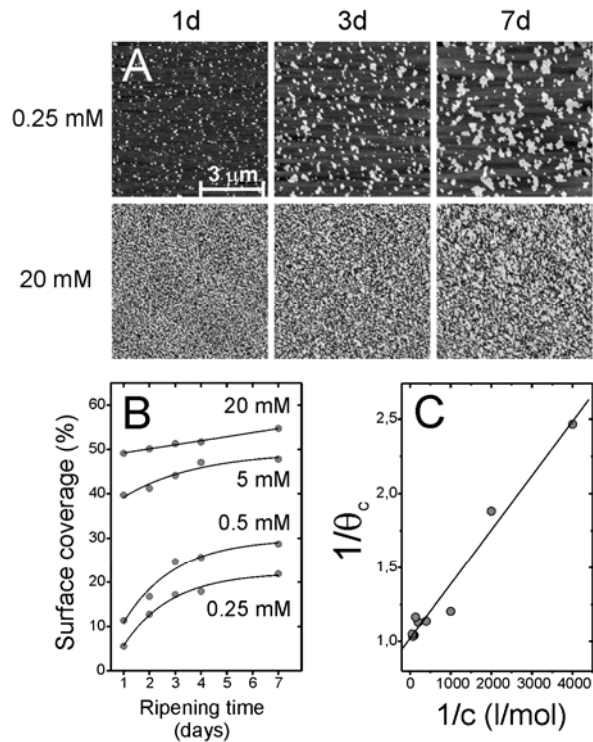


Figure 1. (A) Topographic 6μm x 6μm contact mode AFM images showing the formation and time evolution (ripening) of octadecylamine SAM islands on mica prepared from 0.25mM and 20mM solutions. (B) Evolution of the visible coverage (from island area) as a function of time for various concentrations of the preparation solution. (C) Langmuir type relationship between the relative surface coverage (θ_c) and the concentration of the preparation solution.

Figure 2

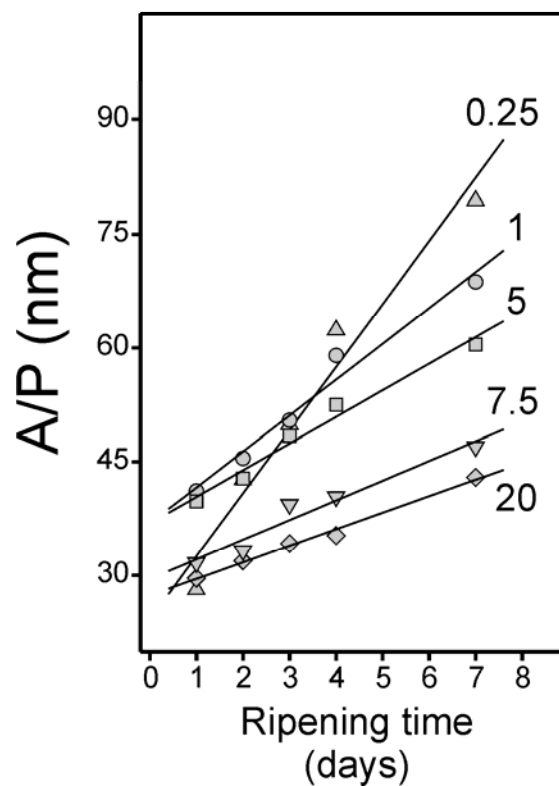


Figure 2. Area-to-perimeter ratio increment of octadecylamine SAM islands describing the island aggregation stage while ripening in air. The slope of the linear plots indicate that the process is faster if prepared from lower concentration solutions.

Figure 3

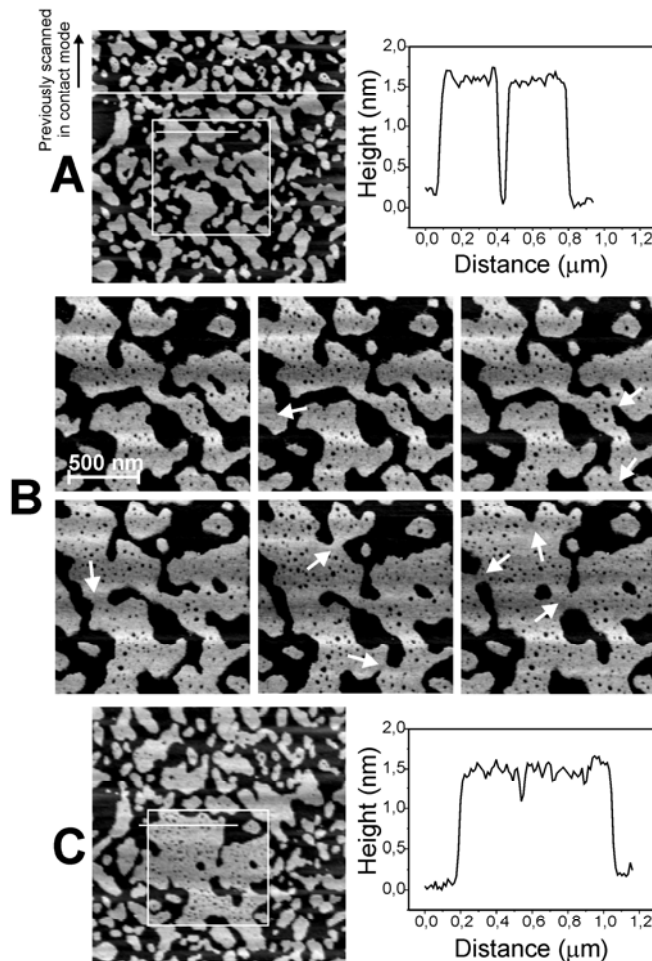


Figure 3. Topographic AFM image obtained in jumping mode showing octadecylamine SAM islands on mica. The top 25% of the image (above white horizontal line) was previously scanned in contact mode at an applied load of 0.5nN. The area inside the white square was later scanned repeatedly in jumping mode at a set point load of 2nN. This resulted in the formation of pinholes and island growth as shown (see arrows) in (B). The images correspond to 11, 15, 19, 21, 27 and 33 accumulated scans respectively (in each scans, every point is sampled four times). The larger image in (C), obtained at a low jumping set point load of 0.5nN after the images in (B), reveals the induced island aggregation and increased pinhole formation. The line profile on the right shows that no modification of the island height occurred.

Figure 4

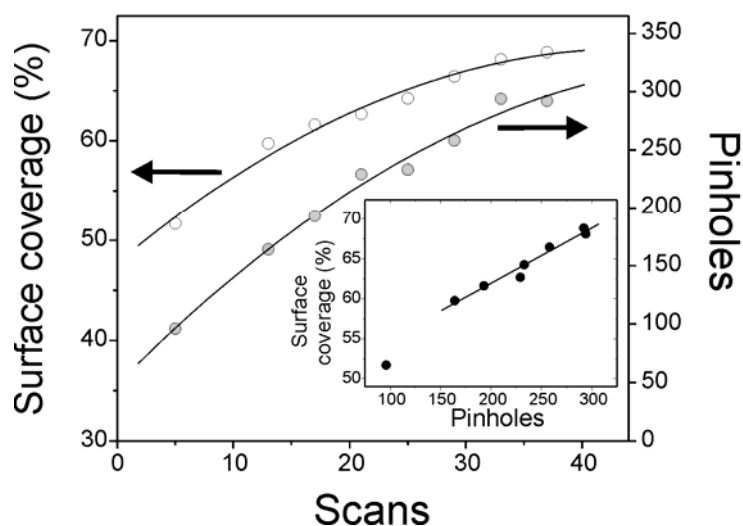


Figure 4. Evolution of surface coverage and number of pinholes created as a function of accumulated scans in jumping mode from the experiments in figure 3. The increment in surface coverage and number of pinholes are directly correlated phenomena (inset).

Figure 5

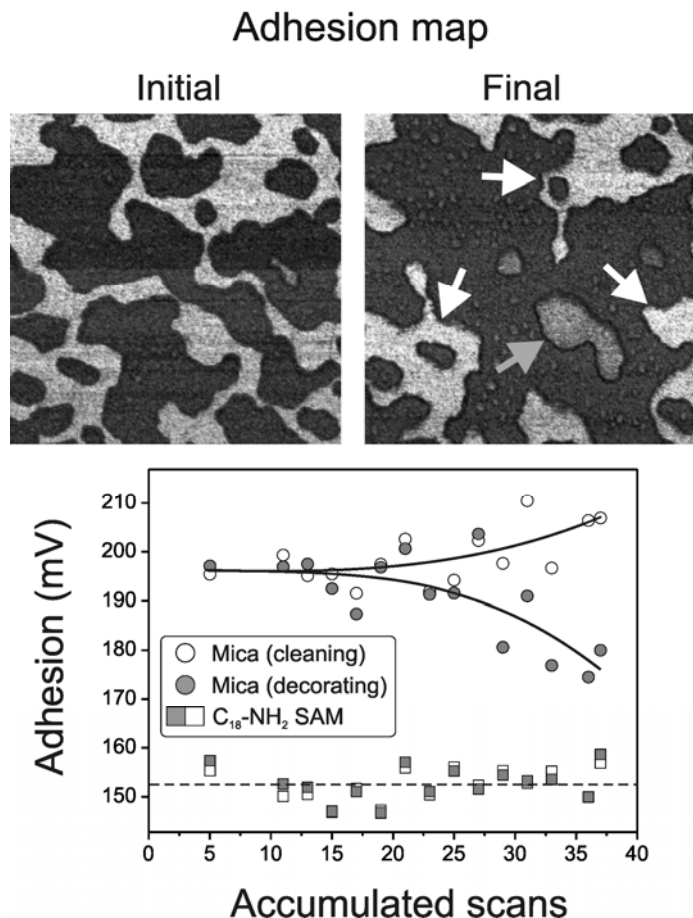


Figure 5. Adhesion force maps corresponding to the initial and final states of the successive jumping mode scanning experiment on octadecylamine SAMs on mica. Two different patterns are observed. In the areas indicated by white arrows the adhesion increases. In others, as that indicated by the gray arrow, the adhesion decreases. The first can be explained by the removal of loosely bound alkyl molecules (cleaning). The second can be explained by the increase in the concentration of molecules, either by direct deposition of from the tip to the substrate (decoration) or by detachment and displacement from the surrounding islands. Adhesion values on the islands are also included in the plot and indicate no modification on this phase.

REFERENCES.

¹ Alves, C. A.; Smith, E. L.; Porter, M. D. *J. Am. Chem. Soc.* 1992, **114**, 1222.

² Tamada, K.; Hara, M.; Sasabe, H.; Knoll, W. *Langmuir* 1997, **13**, 1558.

³ Lio, A.; Charych, D. H.; Salmeron, M. *J. Phys. Chem. B* 1997, **101**, 3800.

⁴ Delamarche, E.; Michel, B.; Biebuyck, H. A.; Gerber, C. *Adv. Mater.* 1996, **8**, 719.

⁵ Camillone, N.; Chidsey, C. E. D.; Liu, G.-y.; Putvinsky, T. M.; Scoles, G. J. *J. Chem. Phys.* 1991, **94**, 8493.

⁶ Strong, L.; Whitesides, G. M. *Langmuir* 1998, **4**, 546.

⁷ Peanasky, J.; Schneider, H. M.; Granick, S.; Kessel, C. R. *Langmuir* 1995, **11**, 953.

⁸ Tidswell, I. M.; Rabedeau, T. A.; Pershan, P. S.; Kosowsky, S. D.; Folkers, J. P.; Whitesides, G. M. *J. Chem. Phys.* 1991, **95**, 2854.

⁹ Xiao, X.-d.; Liu, G.-y.; Charych, D. H.; Salmeron, M. *Langmuir* 1995, **11**, 1600.

¹⁰ Dubois, L. H.; Unzo, R. G. *Annu. Rev. Phys. Chem.* 1992, **43**, 437.

¹¹ Ulman, A. *Chem. Rev.* 1996, **96**, 1533.

¹² Benítez, J. J.; Kopta, S.; Ogletree, D. F.; Salmeron, M. *Langmuir* 2002, **18**, 6096.

¹³ Barrena, E.; Kopta, S.; Ogletree, D. F.; Charych, D. H.; Salmeron, M. *Phys. Rev. Lett.* 1999, **82**, 2880.

¹⁴ Salmeron, M. *Tribol. Lett.* 2001, **10**, 69.

¹⁵ Benítez, J. J.; Kopta, S.; Díez-Pérez, I.; Sanz, F.; Ogletree, D. F.; Salmeron, M. *Langmuir* 2003, **19**, 762.

¹⁶ Benítez, J. J.; Salmeron, M. *J. Chem. Phys.* 2006, **125**, 044708.

¹⁷ Benítez, J. J.; Salmeron, M. *Surf. Sci.* 2006, **600**, 1326.

¹⁸ Moreno-Herrero, F.; Colchero, J.; Gómez-Herrero, J.; Baró, A. M. *Phys. Rev. E* 2004, **69**, 031915.

¹⁹ Horcas, I.; Fernandez, R.; Gomez-Rodriguez, J. M.; Colchero, J.; Gomez-Herrero, J.; Baro, A. *Rev. Sci. Instrum.* 2007, **78**, 013705.

²⁰ Benítez, J. J.; Heredia-Guerrero, J. A.; Serrano, F. M.; Heredia, A. *J. Phys. Chem. C* 2008, **112**, 16968.